NARMAX approach to the Space Weather forecast: results and capabilities

M. A. Balikhin, R. J. Boynton, S. N. Walker

University of Sheffield, UK.

This project has received funding from the European Union's Horizon 2020 research and innovation programme under grant agreement No 637302.

PROGRESS

Introduction to System Identification and NARMAX

Modelling
System identification approach

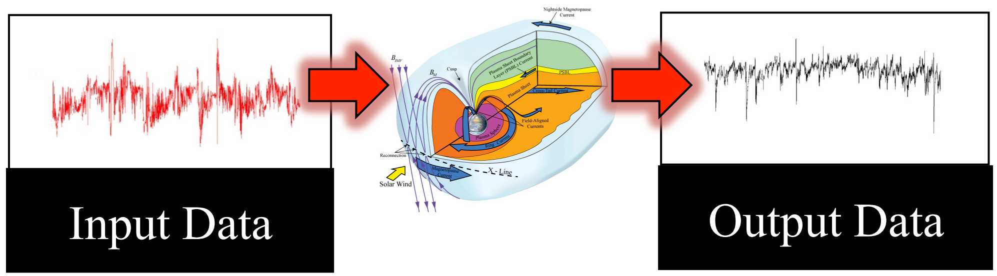

Modelling
System identification approach

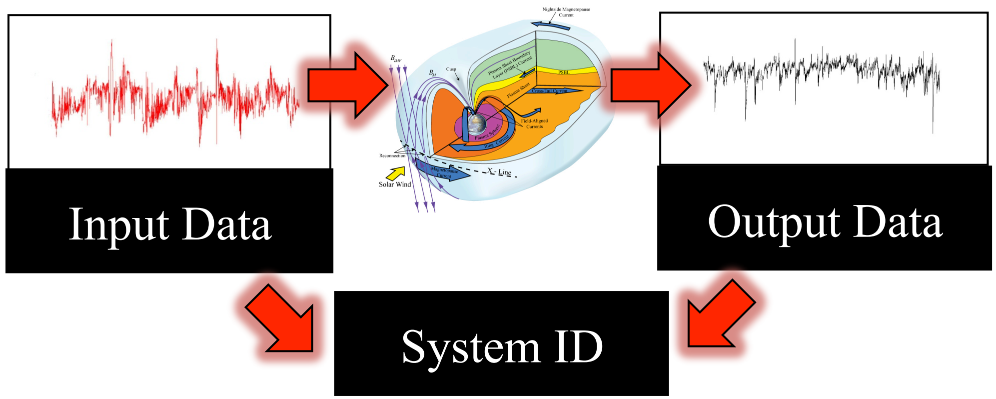

Modelling
System identification approach

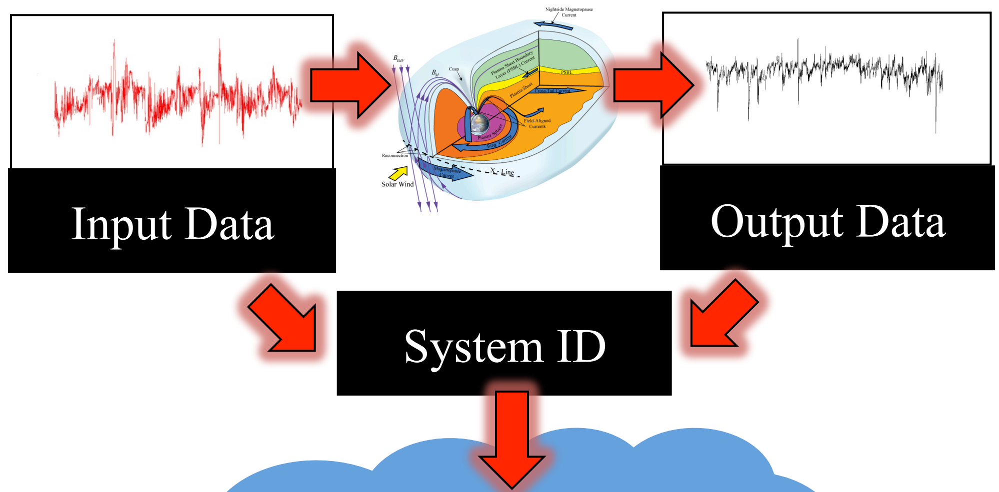

$$S = \int L(x,\dot{x},t)\,dt$$

$$dL = \sum_i \frac{\partial L}{\partial x_i} dx_i + \sum_i \frac{\partial L}{\partial \dot{x}_i} d\dot{x}_i$$

Modelling
System identification approach

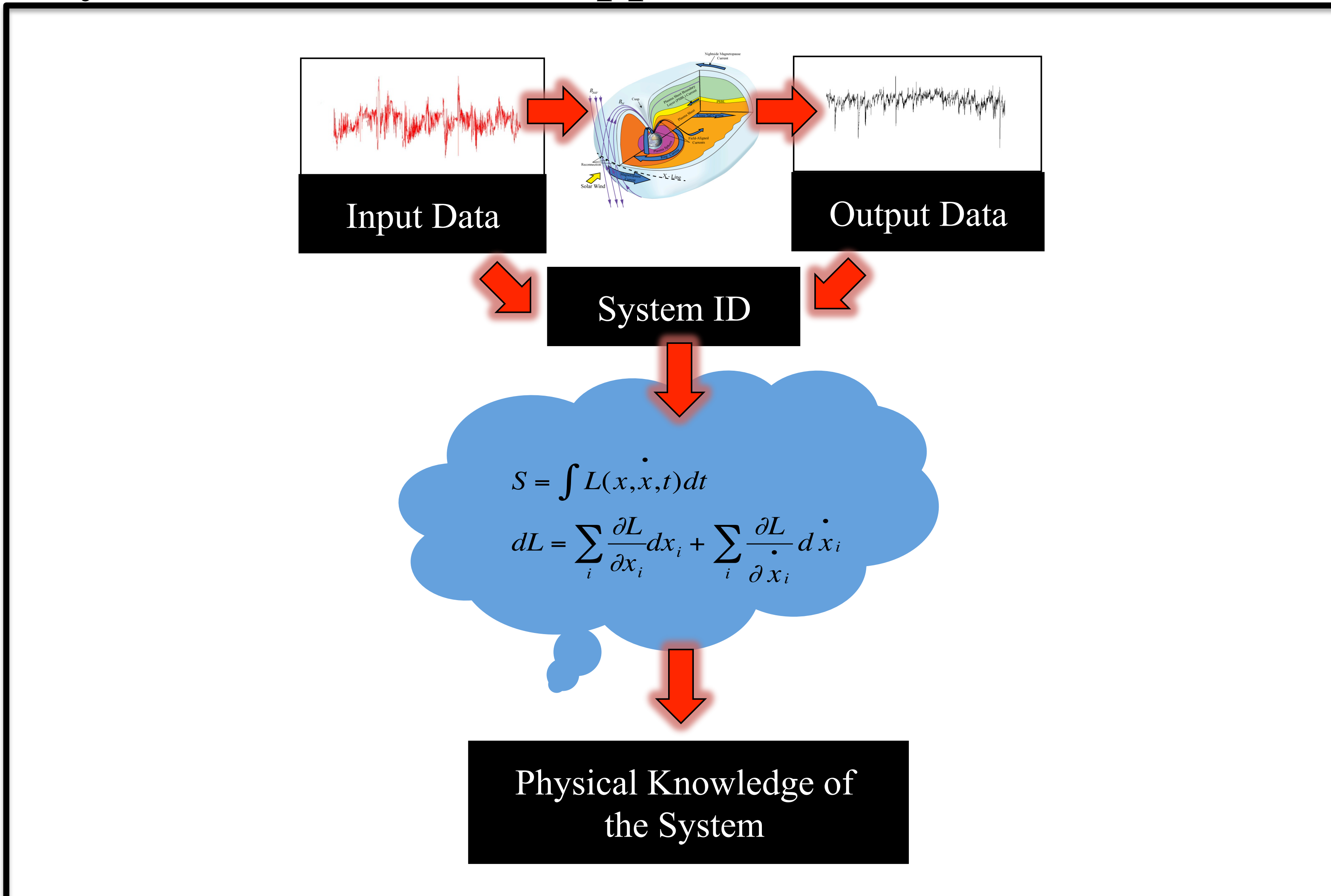

System Identification

Input to the system, u(t) **System** **Output measurement, y(t)**

System Identification

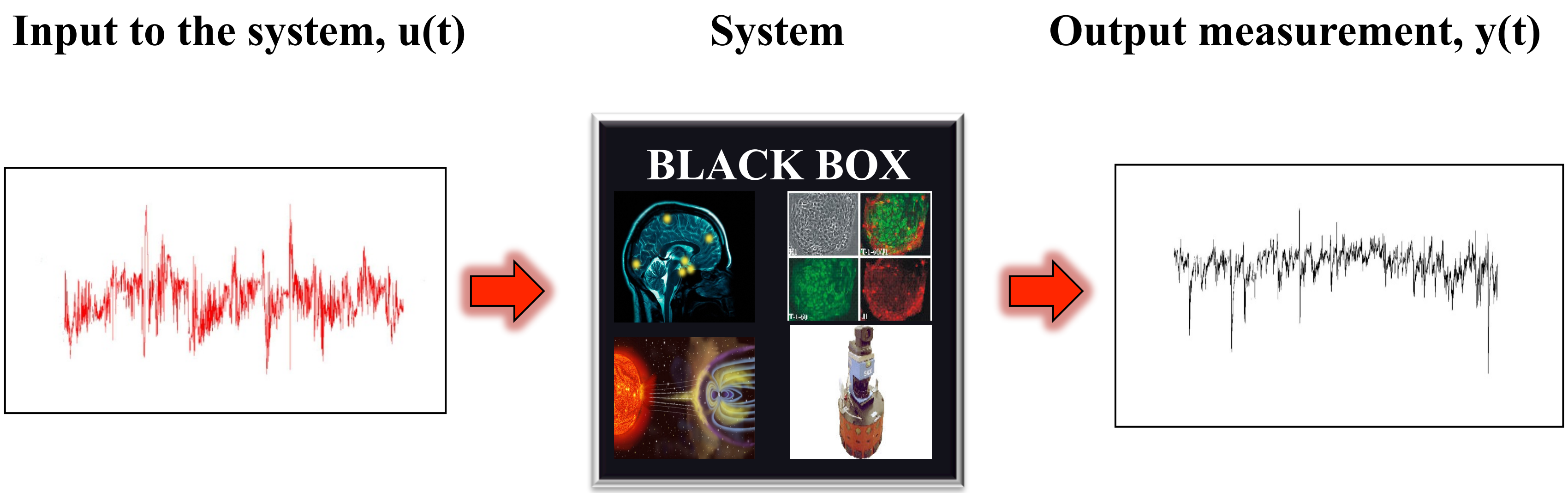

Mapping the input to the output

- Neural Networks
- Genetic Algorithms
- Linear Prediction Filters
- NARMAX – Physically Interpretable

NARMAX

Nonlinear

$$\boxed{\begin{aligned} y(t) = F[&y(t-1),\ldots y(t-n_y), \\ &u_1(t-1),\ldots,u_1(t-n_{u_1}),\ldots, \\ &u_m(t-1),\ldots,u_m(t-n_{u_m}), \\ &e(t-1),\ldots,e(t-n_e)] + e(t) \end{aligned}}$$

NARMAX

Nonlinear **AutoR**egressive

$$\boxed{\begin{aligned} y(t) = F[\, & y(t-1), \ldots y(t-n_y), \\ & u_1(t-1), \ldots, u_1(t-n_{u_1}), \ldots, \\ & u_m(t-1), \ldots, u_m(t-n_{u_m}), \\ & e(t-1), \ldots, e(t-n_e)] + e(t) \end{aligned}}$$

NARMAX

Nonlinear **A**uto**R**egressive **M**oving **A**verage

$$\boxed{\begin{aligned} y(t) = F[\,& y(t-1),\ldots y(t-n_y), \\ & u_1(t-1),\ldots,u_1(t-n_{u_1}),\ldots, \\ & u_m(t-1),\ldots,u_m(t-n_{u_m}), \\ & e(t-1),\ldots,e(t-n_e)] + e(t) \end{aligned}}$$

NARMAX

Nonlinear **A**uto**R**egressive **M**oving **A**verage with e**X**ogenous inputs

$$
\begin{aligned}
y(t) = F[\,& y(t-1),\ldots y(t-n_y), \\
& u_1(t-1),\ldots,u_1(t-n_{u_1}),\ldots, \\
& u_m(t-1),\ldots,u_m(t-n_{u_m}), \\
& e(t-1),\ldots,e(t-n_e)] + e(t)
\end{aligned}
$$

NARMAX

Nonlinear **A**uto**R**egressive **M**oving **A**verage with e**X**ogenous inputs

$$
\boxed{
\begin{aligned}
y(t) = F[\,& y(t-1),\ldots y(t-n_y), \\
& u_1(t-1),\ldots,u_1(t-n_{u_1}),\ldots, \\
& u_m(t-1),\ldots,u_m(t-n_{u_m}), \\
& e(t-1),\ldots,e(t-n_e)] + e(t)
\end{aligned}
}
$$

NARMAX Model:

- Nonlinear Function *F*. e.g. Polynomial, Wavelets, etc.
  - Degree of polynomial
  - Type of wavelet
- Inputs
- System lags

NARMAX

Nonlinear AutoRegressive Moving Average with eXogenous inputs

$$
\begin{aligned}
y(t) = F[\,& y(t-1),\ldots y(t-n_y), \\
& u_1(t-1),\ldots,u_1(t-n_{u_1}),\ldots, \\
& u_m(t-1),\ldots,u_m(t-n_{u_m}), \\
& e(t-1),\ldots,e(t-n_e)] + e(t)
\end{aligned}
$$

NARMAX Model:

- Nonlinear Function *F*. e.g. Polynomial, Wavelets, etc.
  - Degree of polynomial
  - Type of wavelet
- Inputs
- System lags

Polynomial

- FROLS algorithm

  Involves three stages

  1. Structure selection: Error Reduction Ratio (ERR)
  2. Coefficient estimation
  3. Model validation

What solar wind parameters drives Dst index evolution?

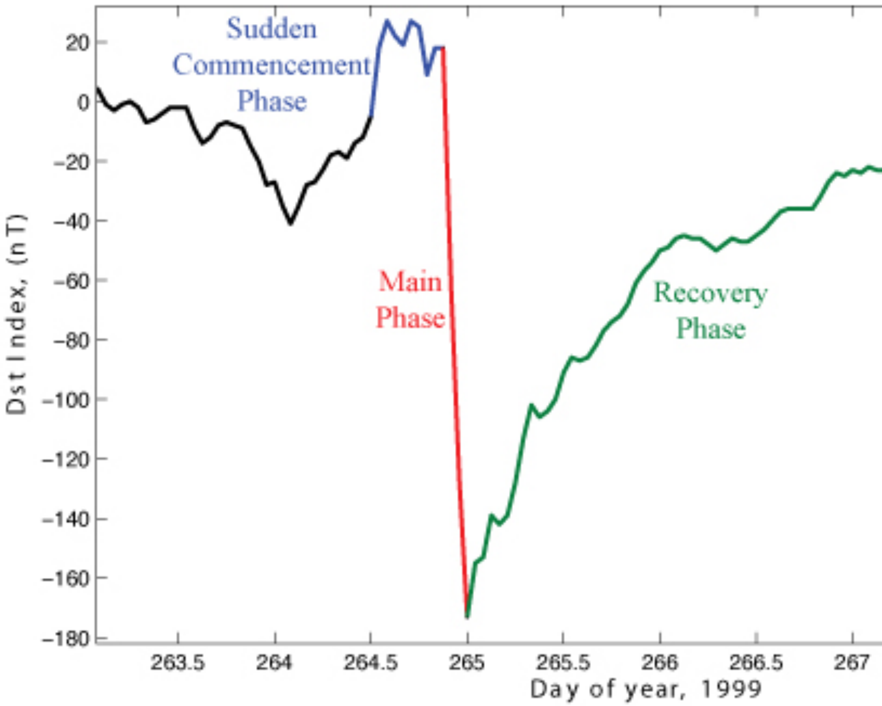

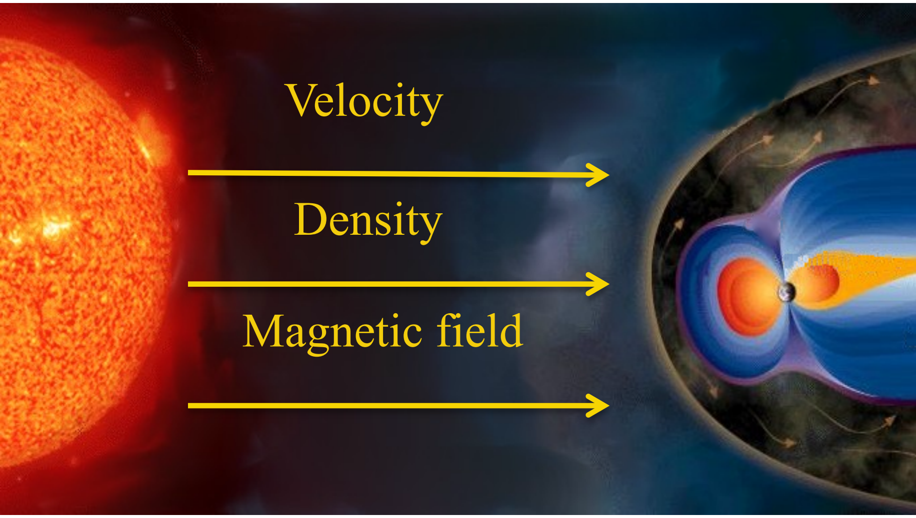

Functional Form	Reference
B_z	*Dungey* [1961]
v	*Crooker et al.* [1977]
n	
$nv^2/2$	*Chapman and Ferraro* [1931]
B_z $(B_z < 0)$; 0 $(B_z > 0)$	
vBs	*Burton et al.* [1975]
$vB^2\sin^4(\theta_c/2)$	*Perrault and Akasofu* [1978]
$vB_T^2\sin^4(\theta_c/2)$	Variant on ε
$vB\sin^4(\theta_c/2)$	Variant on ε
vB_T	
$vB_T\sin^2(\theta_c/2)$	*Kan and Lee* [1979]
$[vB_T\sin^2(\theta_c/2)]^{1/2}$	Variant on the Kan-Lee electric field
$v^{4/3}B_T\sin^2(\theta_c/2)p^{1/6}$	*Vasyliunas et al.* [1982]
$vB_T\sin^4(\theta_c/2)$	*Wygant et al.* [1983]
$[vB_T\sin^4(\theta_c/2)]^2$	Variant on E_{WAV}
$[vB_T\sin^4(\theta_c/2)]^{1/2}$	Variant on E_{WAV}
$v^{4/3}B_T\sin^4(\theta_c/2)p^{1/6}$	*Vasyliunas et al.* [1982]
$vB_T\sin^4(\theta_c/2)p^{1/2}$	*Scurry and Russell* [1991]
$n^{1/2}v^2B_T\sin^6(\theta_c/2)$	*Temerin and Li* [2006]
$v^{4/3}B_T^{2/3}\sin^{8/3}(\theta_c/2)$	Newell et al. [2008]

NARMAX deduced coupling functions

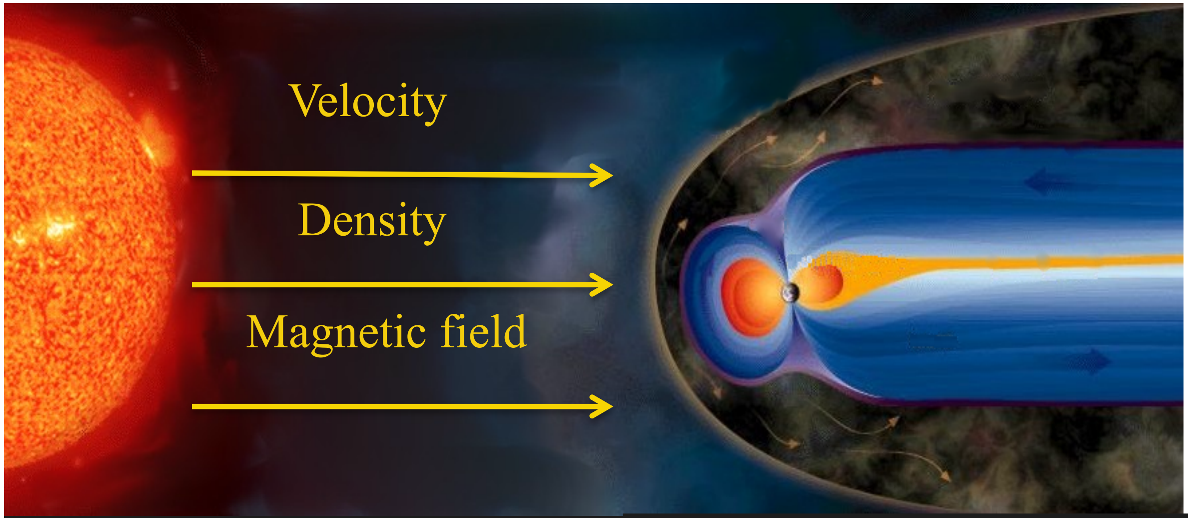

Inputs	Outputs
$p^{1/2}$	Dst
$n^{1/6}$	
$V^{4/3}$	
V	
B_T	
B_s	
$\sin^4(\theta/2)$	
$\sin^2(\theta/2)$	

Expand Nonlinear Function F to a 4^{th} degree polynomial

NARMAX deduced coupling functions

ERR Identified Coupling Function
$p^{1/2}V^2B_T\sin^6(\theta/2)(t\text{-}1)$
$p^{1/2}V^{4/3}B_T\sin^6(\theta/2)(t\text{-}1)$
$n^{1/6}V^{4/3}B_T\sin^6(\theta/2)(t\text{-}1)$

Boynton et al., JGR, 2011

$$\boxed{C_B = p^{\frac{1}{2}}V^2B_T\sin^6\left(\frac{\theta}{2}\right)}$$

Kan and Lee, GRL 1979

$$\boxed{C_{KL} = \frac{V^2}{R}B_T^2\sin^4\left(\frac{\theta}{2}\right)}$$

$$\boxed{\sin^6\left(\frac{\theta}{2}\right)} \quad \text{OR} \quad \boxed{\sin^4\left(\frac{\theta}{2}\right)} \quad ?$$

Analytical justification of the function

Kan and Lee, GRL, 1979

The potential difference Φ_m across the polar cap is due to the perpendicular component of the reconnection electric field, i.e., $E_R \sin \theta/2$ as shown in Figure 1(b). This geometrical factor has been overlooked in the previous studies of component reconnection. Thus the polar cap potential Φ_m can be written as

$$\Phi_m = V_s B_s \sin^2 (\theta/2)\ \ell_o \qquad (3)$$

where ℓ_o is the effective length of the X line.

The power delivered by the solar wind dynamo is given by

$$P = \Phi_m^2/R = V^2 B^2 \sin^4 (\theta/2)\ \ell_o^2/R$$
$$= (V/R)\ \varepsilon(t) \qquad (5)$$

$$E_r = VB\sin(\theta/2)$$

$$E_{r\perp} = E_r \sin(\theta/2)$$

Potential difference

$$\varphi = E_{r\perp} l_o \sin(\theta/2) = VB\sin^3(\theta/2) l_o$$

Power delivered by the solar wind dynamo

$$P = \frac{\varphi^2}{R} = \frac{V^2B^2}{R}\sin^6(\theta/2) l_o$$

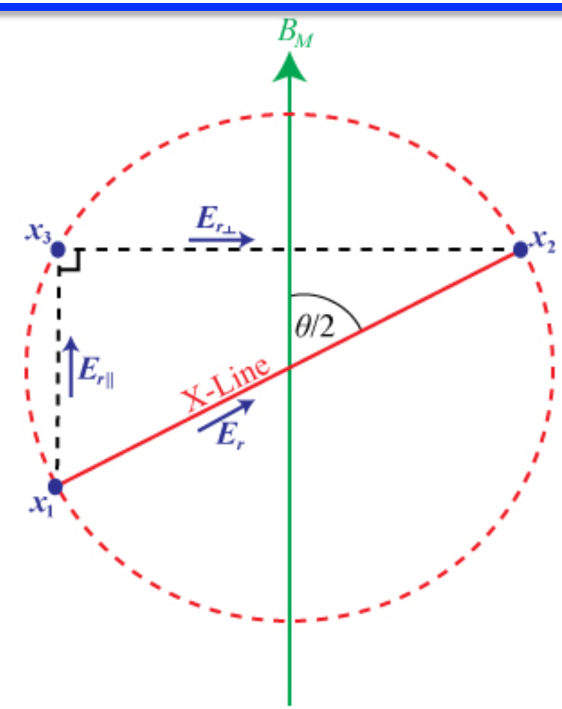

Space Weather Forecasting: GOES Electron Flux Models

Inputs Data

Velocity, Density, pressure, the Dst Index, and southward IMF

Output Data

GOES EPEAD Electron Fluxes

>800 keV Electron Flux

>2 MeV Electron Flux

Electron flux models – SNB3GEO

>800 keV Electron flux model at geosynchronous orbit

PE = 0.700 and CC = 0.847
for 18 months of data
between 01/01/2011
30/06/2012

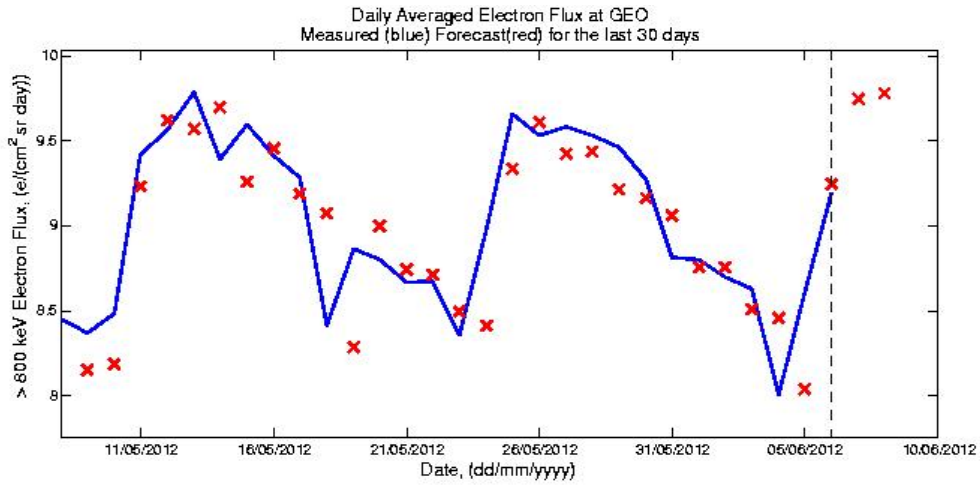

>2 MeV Electron flux model at geosynchronous orbit

PE = 0.786 and CC = 0.894
for over 26 months of data
between 14/04/2010 to
30/06/2012

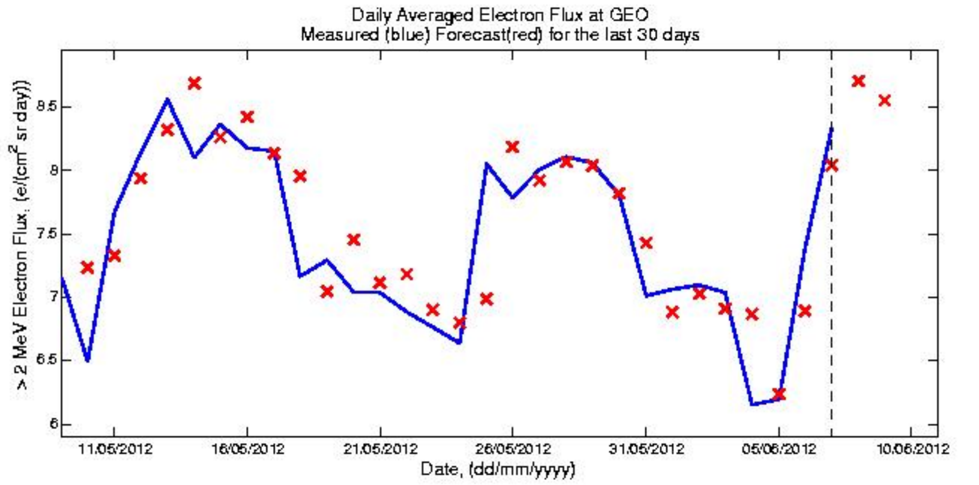

Electron Flux Model – SNB^{3}GEO

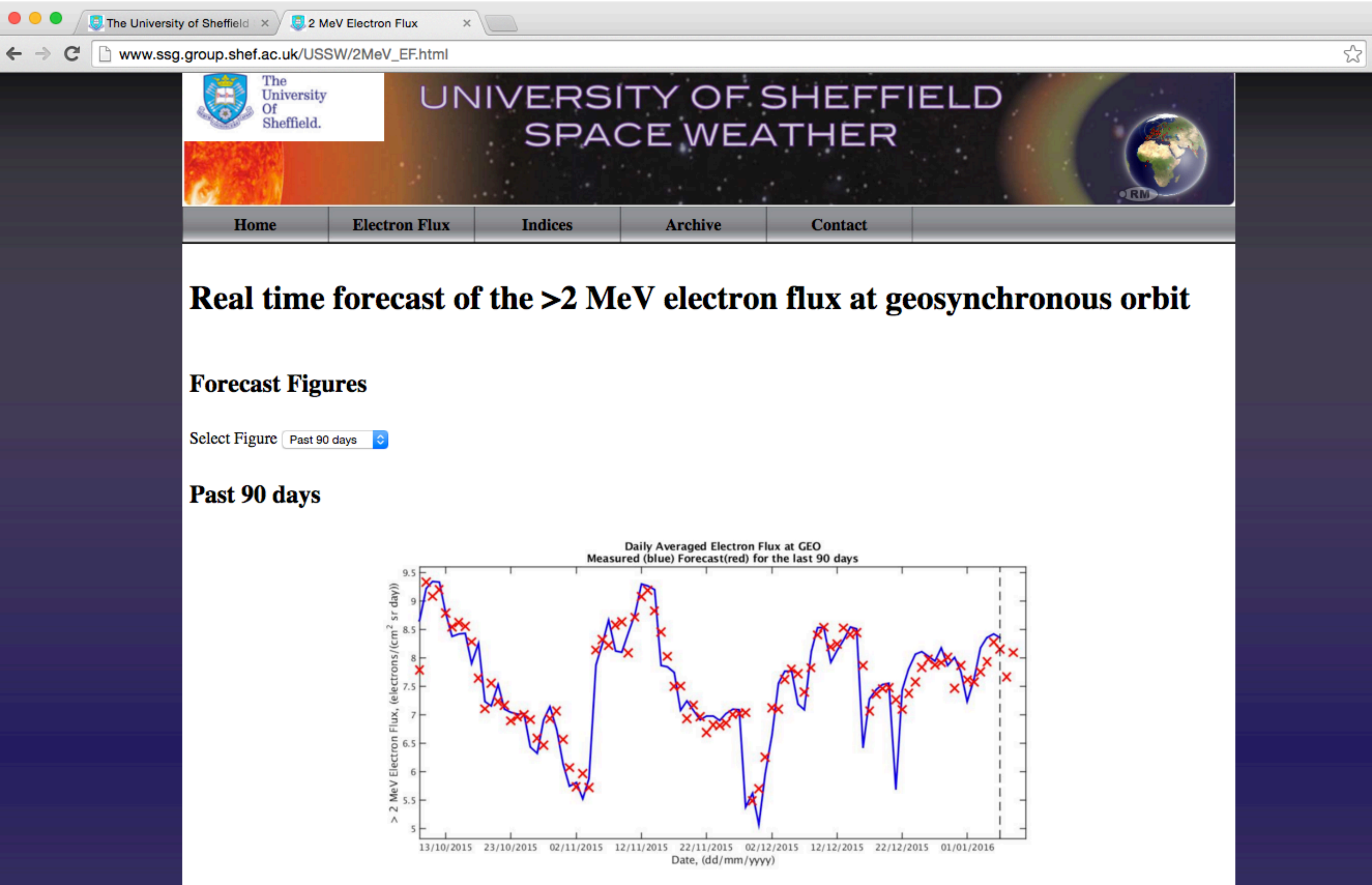

Electron flux – SNB³GEO

NOAA-REFM vs. SNB³GEO

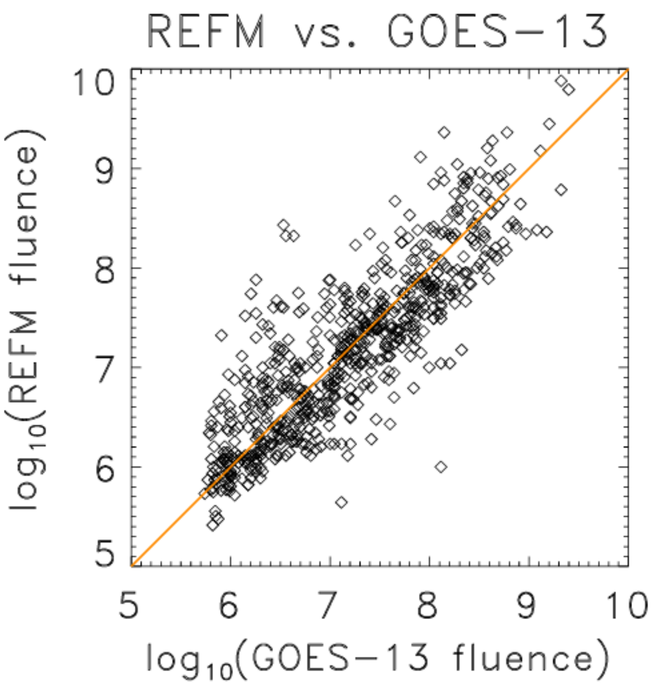

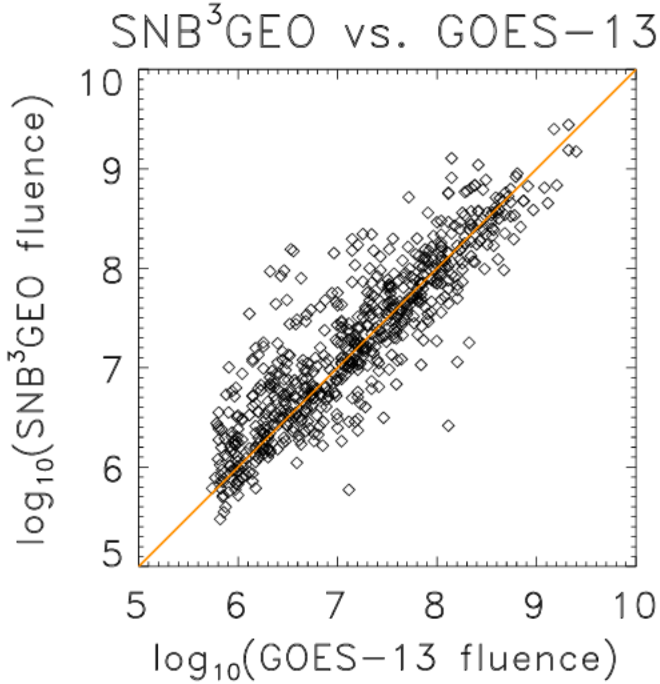

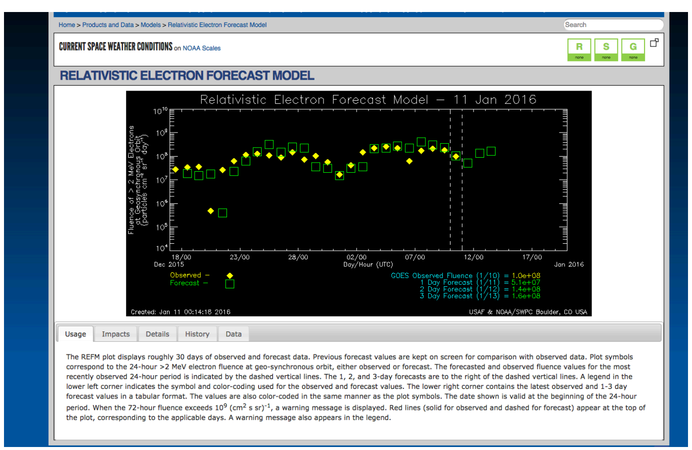

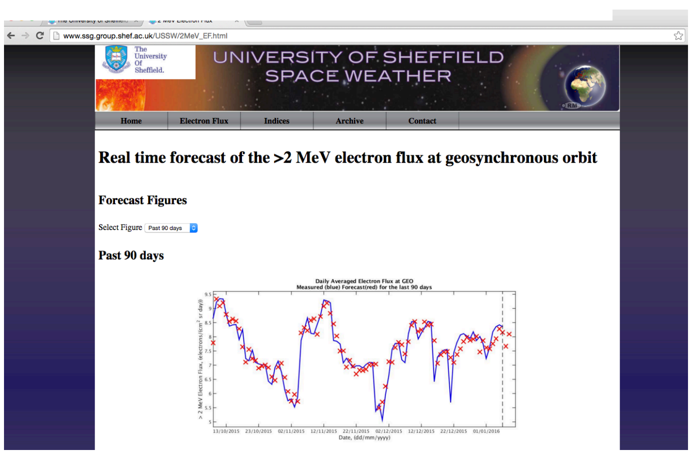

Statistical Analysis of the Model Performance

Prediction Efficiency

$$PE = 1 - \frac{\sum_{t=1}^{N}\left[\left(y(t) - \hat{y}(t)\right)^2\right]}{\sum_{t=1}^{N}\left[\left(y(t) - \overline{y}(t)\right)^2\right]}$$

Correlation coefficient

$$CC = \frac{\sum_{t=1}^{N}\left[\left(y(t) - \overline{y}(t)\right)\left(\hat{y}(t) - \overline{\hat{y}}(t)\right)\right]}{\sqrt{\sum_{t=1}^{N}\left[\left(y(t) - \overline{y}(t)\right)^2\right]\sum_{t=1}^{N}\left[\left(\hat{y}(t) - \overline{\hat{y}}(t)\right)^2\right]}}$$

Where $y(t)$ is the measured output at time t, $\hat{y}$ is the forecast output, N is the length of the data and the bar indicates the mean.

The PE and CC were calculated for each of the model forecasts over the time period shown in the Table below

Electron flux – SNB^{3}GEO

NOAA-REFM vs. SNB^{3}GEO

Balikhin et al. [2016], Space Weather

Fluxes

Model	Correlation	PE
REFM	0.73	-1.31
SNB^{3}GEO	0.82	0.63

$\log_{10}$(Fluxes)

Model	Correlation	PE
REFM	0.85	0.70
SNB^{3}GEO	0.89	0.77

March 2nd, 2012 - January 1st 2014.

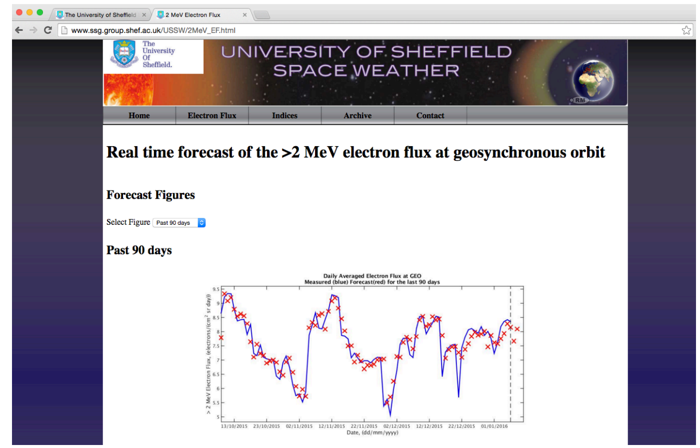

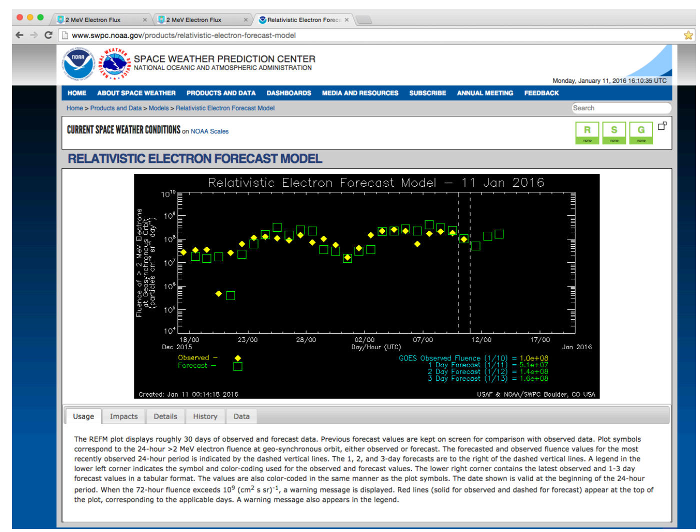

GOES MAGED Energy Models

1. 30-50 keV
2. 50-100 keV
3. 100-200 keV
4. 200-350 keV
5. 350-600 keV

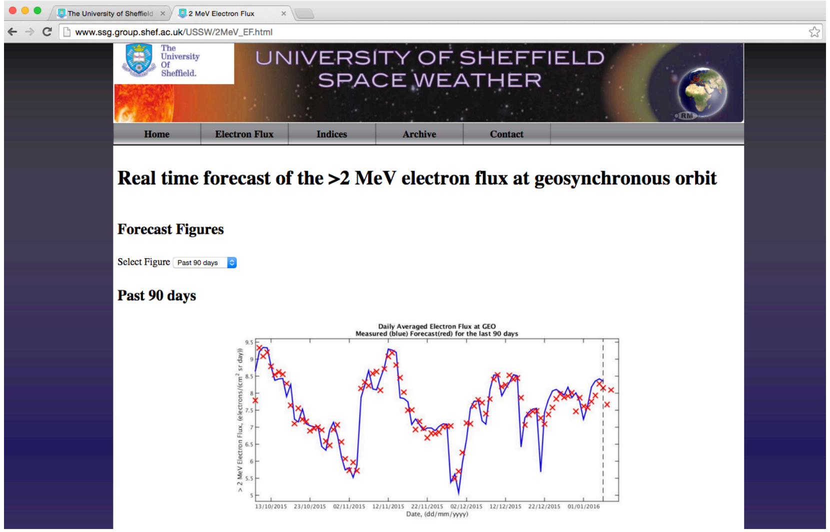

Data

Inputs Data

Velocity, Density, pressure, the Dst Index, and $B_T \sin^6\left(\theta / 2\right)$

The solar wind data were from the Advanced Composition Explorer (ACE) spacecraft positioned at the L1 Lagrange and supplied by the OMNI website for training the model.

Dst was supplied by the World Data Center for Geomagnetism, Kyoto.

Output Data

The output for each of the models are the daily averaged electron flux measurements taken from GOES MagED at GEO and are supplied by NOAA NWS Space Weather Prediction Center.

Data for NARMAX model

Input: The past 24 hour averages were calculated hourly for each input. Therefore, the input time lags in the algorithm, n_{um}, were hourly. For example, the input U(t-10 hours) represents the average of the points between U(t-10 hours) and U(t-34 hours). The training data used lagged inputs from 2 to 48 hours.

Output: For the training data, the 1-minute corrected electron flux values were daily averaged between 00:01:00 UTC and 00:00:00 UTC the next day for each day. The training data employed autoregressive lags for the the previous 2 days, rather than hourly past 24 hour averages to avoid oversampling.

NARMAX model:

$$\boxed{\begin{aligned} J(t) = F[&J(t-24h), J(t-48h),\\ &v(t-2h), v(t-3h), \ldots, v(t-48h),\\ &n(t-2h), n(t-3h), \ldots, n(t-48h),\\ &p(t-2h), p(t-3h), \ldots, p(t-48h),\\ &\ldots,\\ &e(t-24h), e(t-48h)] + e(t) \end{aligned}}$$

Where F was a fourth degree polynomial.

Forecast Time of NARMAX models

The amount of time that the NARMAX model is able to forecast into the future is dependent on the minimum exogenous lag within the final NARMAX model.

For example, if the minimum exogenous lag within the NARMAX model is a velocity value 10 hours ago

$$J(t) = aV(t-10) + \ldots$$

Where a is the coefficient, then if we know the velocity at the present time *t*, then we can calculate an estimate of the electron flux, *J*, at time *t*+10 hours (a 10 hour ahead forecast)

$$J(t+10) = aV(t) + \ldots$$

Model Performance Figures

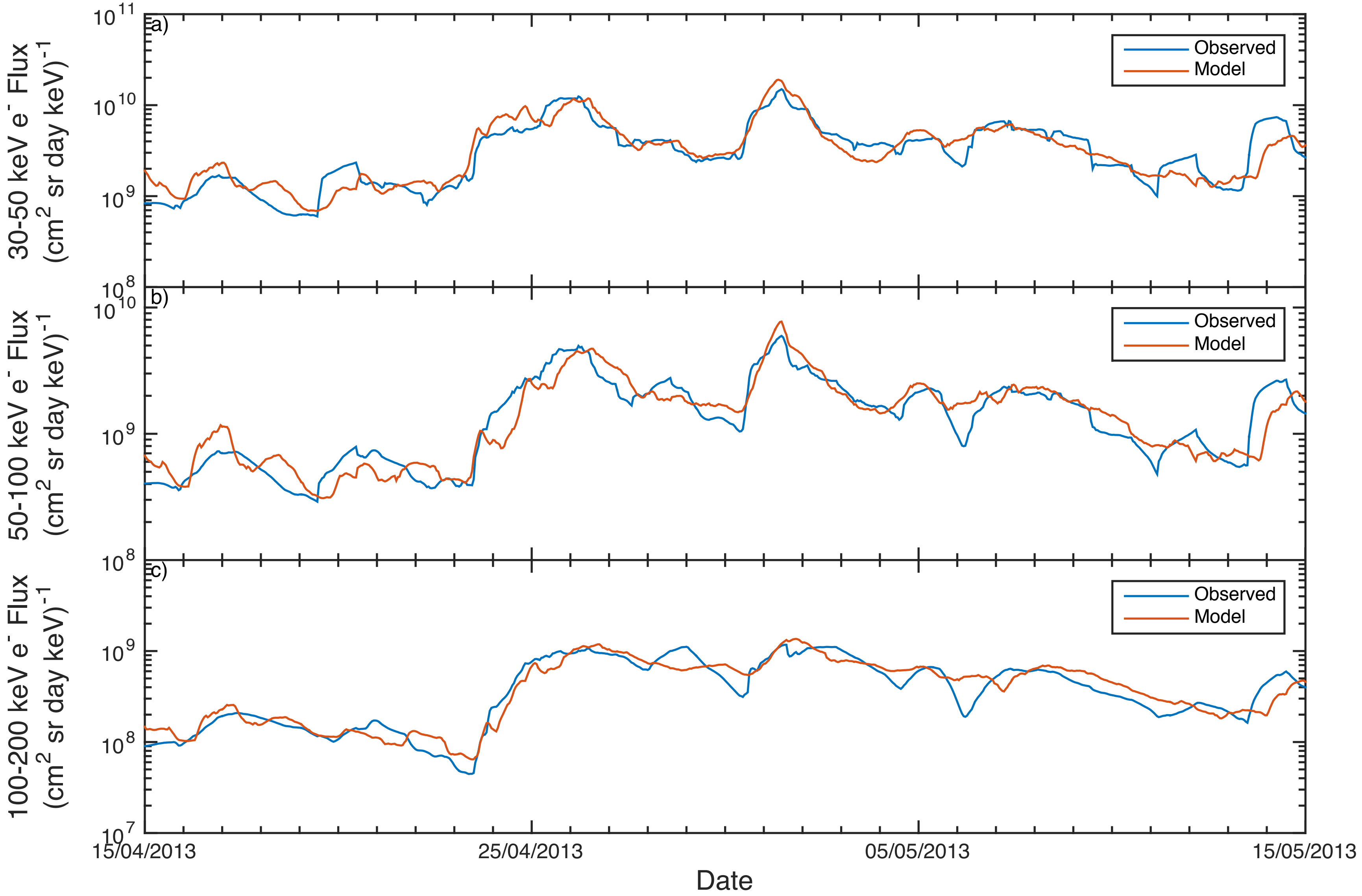

Model Performance Figures

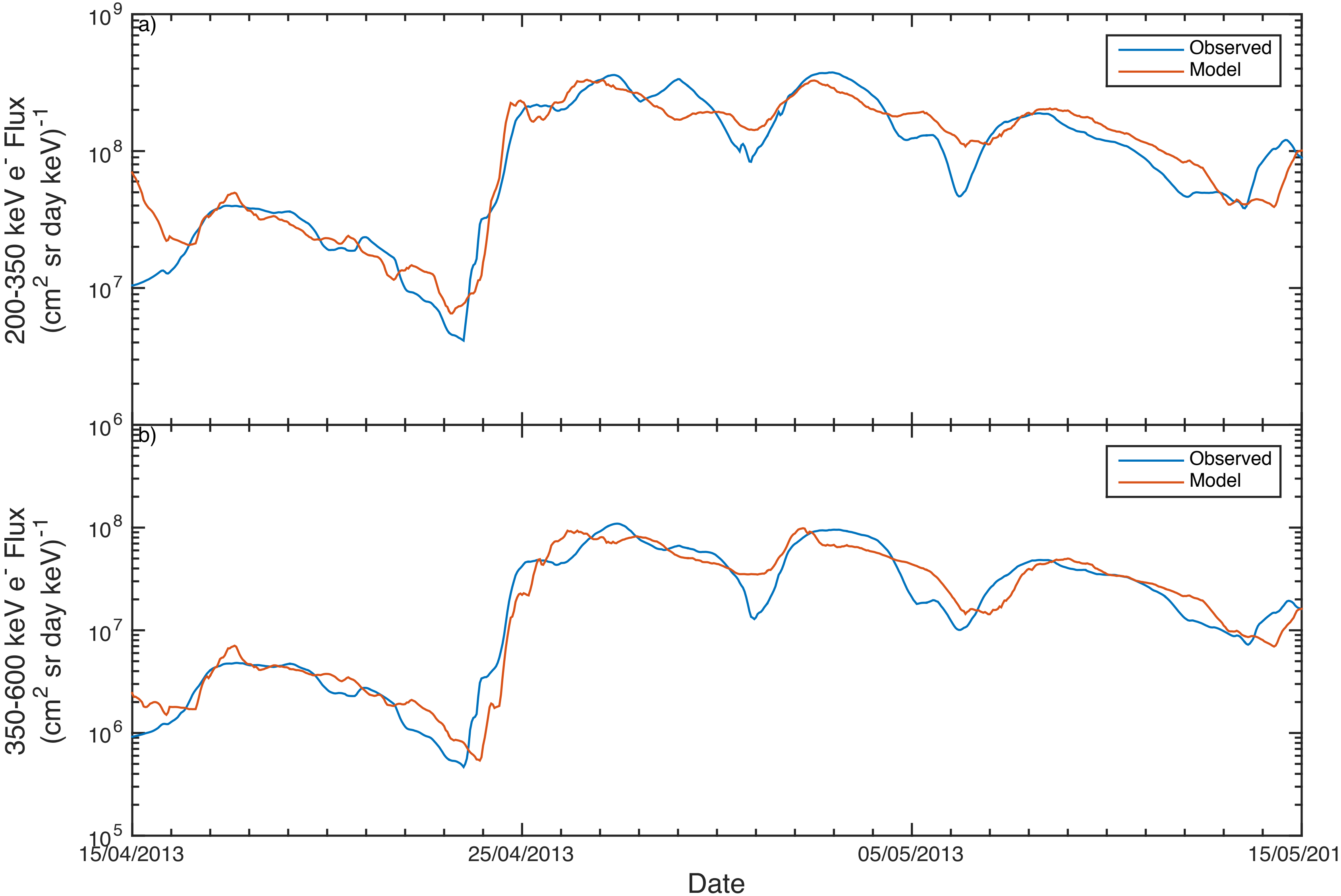

Model Performance Figures

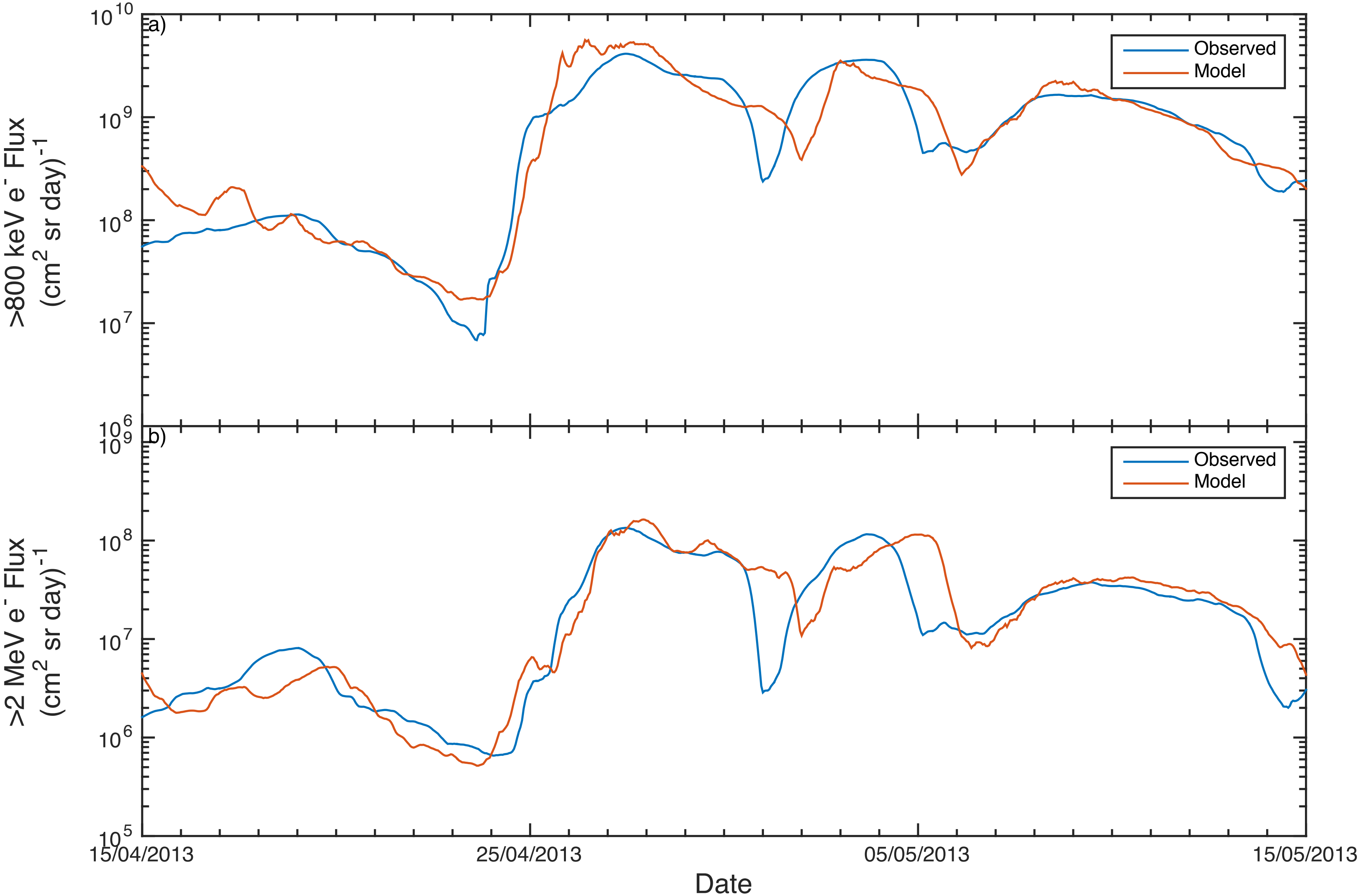

Model	Forecast Time (hours)	PE (%)	CC (%)	Period
40-50 keV	10	66.9	82.0	01.03.2013-28.02.2015
50-100 keV	12	69.2	83.5	01.03.2013-28.02.2015
100-200 keV	16	73.2	85.6	01.03.2013-28.02.2015
200-350 keV	24	71.6	84.9	01.03.2013-28.02.2015
350-300 keV	24	73.6	85.9	01.03.2013-28.02.2015
> 800 keV	24	72.1	85.1	01.01.2011-28.02.2015
> 2MeV	24	82.3	90.9	01.0.12011-28.02.2015

Real-time operation

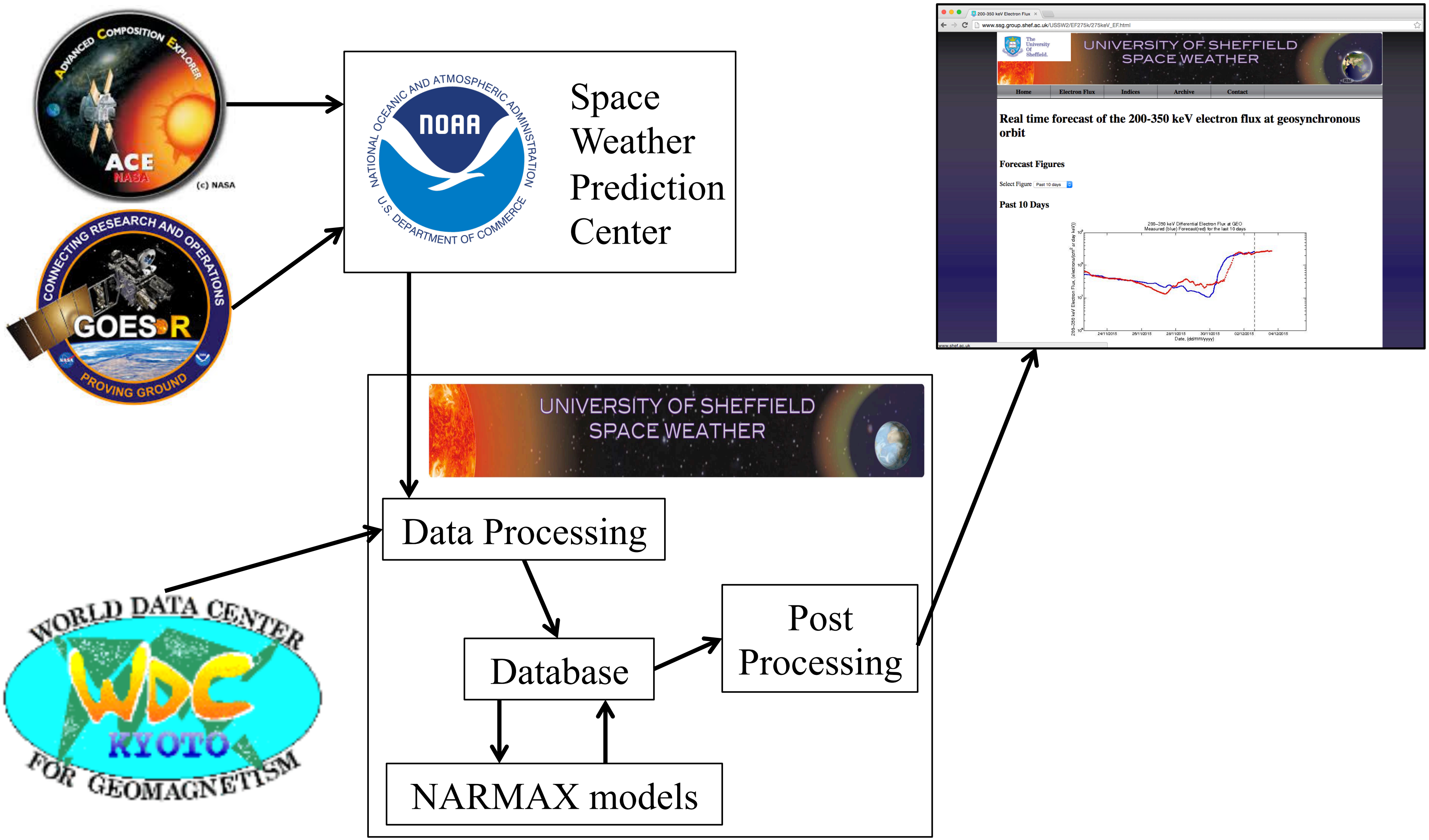

This project has received funding from the European Union's Horizon 2020 research and innovation programme under grant agreement No 637302.